

# 000 COMPACT YET CAPABLE: DO MULTITASK-BASED 001 MULTI-TEACHER DISTILLATION WITH PRECISION- 002 CONTROLLED TASK-SPECIFIC DYNAMIC PTQ 003 OUTPERFORM STATIC QUANTIZATION FOR LOW- 004 RESOURCE MULTITASK NLU?

009 **Anonymous authors**

010 Paper under double-blind review

## 014 ABSTRACT

016 The evolution of conversational AI emphasizes not just accuracy, but also effi-  
017 ciency and scalability. In low-resource Indic languages (Tamil, Telugu, Malay-  
018 alam, Kannada, Hindi, Bengali), cross-domain, multi-intent NLU tasks such as  
019 Intent Detection (ID), Domain Classification (DC), and Slot Filling (SF) be-  
020 come especially challenging due to cross-domain variability and limited annotated  
021 data. LLMs, though powerful, incur high computational costs and slow inference  
022 due to their high resource requirements. Knowledge Distillation (KD) enables  
023 lightweight student models to retain performance from larger teachers, while post-  
024 training quantization (PTQ) further reduces inference cost, making low-resource  
025 multitask NLU more feasible on constrained hardware. In our paper, we investi-  
026 giate scalable deployment architectures for multitask NLU tasks in resource-  
027 constrained environments. We compare static PTQ applied to a non-distilled mul-  
028 titask baseline with precision-controlled, task-specific dynamic PTQ applied to a  
029 multi-teacher based distilled student. Static PTQ uses QuantStub/DeQuantStub,  
030 calibration over representative batches, and zero-point quantization, while af-  
031 ter training, the distilled student undergoes precision-controller-driven dynamic  
032 PTQ. The student is distilled from three pairs of teachers (ID-DC, ID-SF, DC-SF)  
033 using adaptive attention-based fusion and temperature scaling. The controller  
034 assigns different precisions for encoder attention layers, encoder MLP blocks,  
035 and each multitask head (ID, DC, SF), allowing finer-grained accuracy-efficiency  
036 optimization without calibration. By unifying weight and activation precision  
037 under a single runtime policy, our approach further reduces memory and band-  
038 width requirements without degrading accuracy. Experimental results on a custom  
039 multilingual Indic dataset show that our multitask based multi-teacher-distilled,  
040 precision-controller-quantized student achieves a superior accuracy-efficiency  
041 trade-off, significantly reducing inference latency, memory footprint, and runtime  
042 bandwidth while preserving accuracy across NLU tasks. Our study demonstrates  
043 that unifying KD with precision-controlled, task-specific dynamic PTQ under a  
044 single weight-activation policy delivers scalable, real-time NLU for low-resource  
045 multilingual settings while achieving optimal efficiency-accuracy trade-offs.

## 046 1 INTRODUCTION

047 Conversational AI in low-resource Indic languages faces challenges in cross-domain, multitask NLU  
048 due to limited data and domain variability. This paper explores scalable deployment using KD and  
049 PTQ techniques to enable efficient, real-time inference on constrained hardware and low-resource  
050 settings. Fig. 1 shows cross-domain Indic user-utterances expressing multiple intents.

051 **Contributions :**

- 052 • **Static PTQ of Baseline MultiLingual MultiTask Model.** We propose a static PTQ  
053 pipeline tailored specifically for a multilingual, multitask baseline fusion model using

054	Language	User-Utterance	Intents	Domains	Slots
055	Hindi	ਪੰਜਾਬੀ ਢਾਬਾ ਸੇ ਮੇਰੇ ਲਿਖੇ ਇੱਕ ਆਲੂ ਕਾ ਪਰਾਥਾ ਅੰਦਰੋਂ ਕਰੋ। ਮੇਰੇ ਪਾਸ ਥਾਂਡੀ ਸੀ ਫਿਲਿਆ ਹੈ ਮੈਂ ਇਸੇ ਕੋਸ਼ਿਸ਼ ਵਿੱਚਾਂ।   ਟੱਕੋ ਪਕਾਨੇ ਕਾ ਸਵਰਗੀ ਆਰਾਮ ਔਰ ਜਲਦੀ ਰੀਤੀਕਾ ਕਿਵੇਂ ਹੈ।	takeaway_order , cooking_recipe , cooking_query	takeaway , cooking	[business_name : Punjabi Dhaba] O O O [food_type : Potato] O [food_type : Paratha] O O   O O O [food_type : Fish] O O O O O   O O O O O O O O O
056		Order me an aloo ka paratha from Punjabi Dhaba. I have some fish how do I cook it. What is the easiest and quickest way to cook turkey			
057	Bengali	আপনি কি সাড়ে সাতটির ডিনার আমার আলার্ম সেট করতে পারেন। আমি আজ নয়টা মুঠুর রাত একটা তার সাথে দেখা করতে পারি।	alarm_set , calendar_query , email_send	calendar , alarm , email	O O [time : 7:30] O O O O O   O [date : today] [time : nine] O [time : five] O O [event_name : meeting] O O   [person : Shabana] O O O O O [date : Saturday] O [time : one o'clock] O O O O O
058		Can you set my alarm for 7:30?   How many meetings do I have today from 9 to 5?   Send Shabana an email that I can meet her on Saturday at 1 p.m.			
059	Kannada	ದಂಗಲ ಈತಿದ್ದ ಹಾಡನ್ನು, ಡೈನಾಲ್‌ಫೆಡ್‌ ಮಾಡಿ ಯಾವು, ಉಳಿಸಿ. ಮುಳ್ಳಿಸ್ಕ್ ಈ ಈ ಈವೆಲ್‌ ಸೆಂಟ್‌ ರ್ಯಾಂಕ್‌, ಮ್ಯಾಲ್‌ಫೆಡ್‌ ಈವೆಲ್‌. ಡೈನಾಲ್‌ಫೆಡ್‌ ನೀನಿಗೆ ಅಂತರೆ ಜನಹಿಂದಿಗೆ ಡಾಂಗಲ್‌ಫೆಡ್‌ ಅನ್ನು ಹೇಳಿ.	music_likeness , audio_volume_up , play_podcasts	music , play , audio	[music_descriptor : Dangal movie] O O O O O   O [change_amount : To Level Seven] O [device_type : Music Player]   O O O O O O O O O
060		Download and save Dangal movie song. Music to Level Seven Music Player. Play the most popular podcast for me on iTunes.			
061					
062					
063					

Figure 1: Examples of User Utterances with Multiple Intents Across Domains in Indic Low-Resource Languages

QuantStub/DeQuantStub, min-max calibration, and zero-point encoding, resulting in an int8 model that reduces memory and speeds up CPU inference with minimal performance loss on low-resource cross-domain, multi-intent Indic NLU tasks catering to 6 Indic Languages (Bengali, Hindi, Tamil, Telugu, Kannada, Malayalam).

- **Dynamic PTQ of MultiLingual Distilled Model.** We introduce a multitask, multi-teacher distillation framework designed for 6 Indic languages where three specialized teacher models (ID+DC, DC+SF, ID+SF) jointly transfer task-specific knowledge to a unified student model. The student employs attention-based fusion to dynamically prioritize informative teacher signals and integrates adaptive temperature scaling and contrastive learning to improve cross-task generalization. After training, we apply dynamic post-training quantization, converting all linear components, including attention and task-specific layers, into int8 without calibration, resulting in a highly efficient model with strong NLU performance.
- **Precision Controlled Task Specific Dynamic PTQ under unified weight-activation policy** We propose a novel precision-controller-driven task specific dynamic PTQ scheme that jointly quantizes weights and activations. At deployment, the controller selects and freezes bit-widths from 4, 8, 16 independently for encoder attention layers, encoder MLP/linear blocks, and each NLU task head. Built on a multitask based multi-teacher KD framework, our approach produces compact, efficient student models that permanently reduce memory footprint and inference latency while preserving accuracy in low-resource, multilingual, multitask NLU settings.

## 2 LITERATURE SURVEY

Recent advancements in multitask NLU, knowledge distillation (KD), and quantization have informed our approach. Saha et al. (2021) proposed a BERT-based multitask framework for joint modeling of Domain Classification (DC), Intent Detection (ID), and Slot Filling (SF) leveraging capsule networks and conditional random fields. Knowledge distillation techniques such as soft-probability transfer by Hinton et al. (2015) and intermediate-layer hints in FitNets by Romero et al. (2014) motivate the multi-teacher distillation strategies used in this work. MIDAS, a multi-level, multi-teacher KD framework for multi-turn NLU that improves ID, SF and DC, was proposed by Li et al. (2024). In the quantization domain, several notable approaches have shaped best practices for post-training quantization (PTQ) and low-bit deployment. Jung et al. (2019) optimized quantization intervals via task-loss-driven learning to preserve accuracy under static quantization, and Frantar et al. (2022) introduced GPTQ, an accurate post-training quantization method for large transformers. Xiao et al. (2023) proposed SmoothQuant to enable efficient, high-fidelity LLM quantization without retraining. Works such as Lang et al. (2024) and Hu et al. (2023) analyze and compare static, dynamic, and post-training quantization strategies, providing guidance for choosing calibration schemes and per-tensor vs. per-channel formats. Additionally, El-Kurdi et al. (2022) proposed zero-shot dynamic quantization approaches that reduce reliance on calibration data. There is also growing interest in combining KD with quantization. Ranjan & Savakis (2024) apply multi-step KD for vision transformer quantization, while Sun et al. (2021) explore collaborative teacher-student learning across multiple knowledge sources for quantized networks. Liu et al. (2024) investigate evolving KD strategies with large language models and active learning to bridge the performance

108 gap in quantized architectures. Early mixed-precision PTQ methods search per-layer bit-widths  
 109 using hardware or second-order signals. Wang et al. (2019) employs reinforcement learning with  
 110 hardware feedback to learn layer-wise precision policies, showing that non-uniform bit-widths can  
 111 improve efficiency with minimal accuracy loss. Dong et al. (2020) leverage the Hessian spectrum  
 112 to assign mixed precision and determine quantization order, again at layer granularity. For large  
 113 Transformers, Yao et al. (2022) provide end-to-end PTQ pipelines (often combined with knowledge  
 114 distillation) and explore design spaces across bit precisions and model families, however, they do  
 115 not expose per-task-head control at deployment. Addressing activation outliers, Xiao et al. (2023)  
 116 shifts activation difficulty into weights via offline channel-wise scaling. Recent dynamic and task-  
 117 conditioned approaches in Xiao et al. (2025), preserve task-critical weight “circuits” in higher pre-  
 118 cision to sustain accuracy at very low bitwidths. Yet these methods are primarily weight-focused,  
 119 do not unify activation precision under a single policy, and provide no explicit, user-controllable  
 120 per-head knobs. Overall, prior work is typically (i) weight-only or activation-only in practice, (ii)  
 121 optimized at the layer/block level without per-head (ID/DC/SF) control, and/or (iii) missing a uni-  
 122 fied runtime policy that jointly governs both weights and activations. Taken together, these studies  
 123 motivate our design: a multi-teacher KD pipeline tailored to multilingual, multitask NLU, followed  
 124 by precision-controlled dynamic PTQ.

### 3 DATASET

125  
 126 For our experiments, we focus specifically on six low-resource Indic languages - Bengali, Hindi,  
 127 Tamil, Telugu, Kannada, and Malayalam. A custom multi-intent, cross-domain dataset was prepared  
 128 from the MASSIVE benchmark (Jack FitzGerald, 2022). Representative samples are illustrated in  
 129 Fig. 1. This custom data set contains 163,109 training utterances and 40,778 testing utterances that  
 130 span all six languages, annotated with 540 distinct intent labels, 37 domain categories, and 60 slot  
 131 types. Since we are working on a multi-sentence structured dataset, this was the best suited dataset  
 132 that could be potentially leveraged for all our experiments.  
 133

### 4 METHODOLOGY

134  
 135 This section compares static, dynamic, and our proposed precision-controlled PTQ methods, with  
 136 and without KD for cross-domain, multi-intent NLU in low-resource Indic languages, along with  
 137 the detailed experimental setup. We present a unified and efficient multilingual NLU framework  
 138 that uniquely integrates multitask learning, multi-teacher KD, and PTQ to address the challenges of  
 139 low-resource Indic languages. Our approach begins with a multitask learning setup, where a single  
 140 XLM-R model is trained to perform ID, DC and SF jointly which acts as a baseline. To further  
 141 enhance this multitask model, we introduce a multi-teacher distillation strategy. Here, three com-  
 142plementary teacher models—each trained in a subset of tasks (ID+DC, DC+SF, ID+SF) provide  
 143 specialized task-level supervision to a unified student model. The student incorporates attention-  
 144 based fusion to dynamically weigh and integrate teacher output, along with contrastive learning to  
 145 align task and language representations in a shared semantic space. This design allows the student  
 146 to learn simultaneously from multiple tasks and languages, improving its robustness and generaliza-  
 147 tion. After training, we apply PTQ to compress the model for efficient deployment. Static PTQ is  
 148 used on the non-distilled baseline multitask model with affine calibration and zero-point encoding.  
 149 In contrast, the distilled student benefits from dynamic quantization, which converts all linear and  
 150 task-specific layers (including attention and decoder heads) into INT8 format without calibration  
 151 data, preserving flexibility and performance. Building upon this, we introduce our novel precision-  
 152 controlled task-specific dynamic PTQ method. Unlike prior approaches, this technique incorporates  
 153 a learned precision controller that selects bit-widths from 4, 8, 16 separately for encoder attention  
 154 layers, encoder MLP/linear blocks, and each task-specific head (ID, DC, SF). At deployment, the  
 155 controller deterministically freezes precision choices per component, replacing each selected linear  
 156 layer with a Quantized Linear module whose weight tensor is stored in int8/int16/int4, significantly  
 157 reducing model size and memory footprint. At runtime, activations are fake-quantized using the  
 158 same chosen precision, which reduces bandwidth and latency. By unifying weight and activation  
 159 quantization under a single runtime policy, this method achieves both aggressive compression and  
 160 strong accuracy preservation.

162 4.1 STATIC QUANTIZATION ON A MULTITASK MODEL  
163

164 To build the baseline multitask model for cross-domain NLU, we had leveraged XLM-R Model to  
165 generate contextualized hidden state representations for Indic languages, enhancing cross-lingual  
166 understanding in low-resource settings. Each language specific input sequence is tokenized and  
167 Word Embeddings, Sentence Embeddings, and Segment Embeddings are then concatenated and  
168 passed to XLM-R Model. Given an utterance  $U_i$  comprising of  $S_1, S_2, \dots, S_m$  belonging to a  
169 target language family F comprising of  $x_i$  tokens. The output i.e hidden state representations, are  
170 represented as follows:

$$171 \quad \mathbf{H}_{\text{CLS}}, \mathbf{H}_1, \mathbf{H}_2 = XLMR(\mathbf{U}_i, \mathbf{M}) \quad (1)$$

173 After computing the hidden states, static PTQ is applied to produce a compact INT8 version for  
174 downstream tasks from a trained FP32 model through the following. **1. QuantWrapper Insertion**  
175 To enable 8-bit inference, two parameter-free modules—QuantStub and DeQuantStub—are inserted  
176 into the model graph. QuantStub converts floating-point activations to 8-bit integers, while De-  
177 QuantStub restores them to float32. These modules ensure correct placement of quantization and  
178 dequantization operations during calibration and conversion, allowing quantization to be applied  
179 without modifying the model’s original weights.

180 **2. Calibration**

181 We run  $N = 100$  batches through the QuantStub to collect per-tensor extrema. From these  
182 extrema we compute the scale  $s$  and zero-point  $z$  for affine quantization. We chose  $N=100$  be-  
183 cause our ablations showed activation-range estimates, and resultant end-task accuracy-plateau after  
184 75 batches, with negligible gains beyond 100, and because seminal PTQ work demonstrates that  
185 sampling on the order of 100–256 batches yields stable extrema for high-quality 8-bit quantization  
186 without incurring prohibitive calibration cost.

187 **3. Affine Quantization**

188 It maps floating-point values to integers using a linear transformation defined by a scale and zero  
189 point. Each scalar entry of  $H_{\text{quant}}[i]$  (for  $i = 1 \dots n$ , each a vector of length  $d$ ) is mapped to  $\text{int8}$   
190 via:

$$191 \quad H_{\text{quant}}[i] = \text{round} \left( \text{clip} \left( \frac{H[i]}{s} + z, q_{\min}, q_{\max} \right) \right) \quad (2)$$

$$194 \quad H_{\text{quant}} \in \mathbb{Z}_8^{n \times d} \quad (3)$$

196 The quantized hidden state representation  $H_{\text{quant}}$  is passed to task-specific classifiers, where the  
197 pooled output  $H_{\text{quant}}^{[\text{CLS}]}$  is used for ID and DC, and the sequence output is used for SF, each followed by  
198 a linear layer and a Softmax activation to produce the final predictions. The architecture is explained  
199 in Fig. 3.

201 4.2 MULTI-TASK, MULTI-TEACHER BASED ADAPTIVE KNOWLEDGE DISTILLATION  
202

203 We propose a multilingual, multitask framework with three interrelated teacher models (ID+DC,  
204 DC+SF, ID+SF), each built on XLM-R and trained independently to guide a unified student model.  
205 The student employs an attention-based fusion mechanism to dynamically integrate teacher knowl-  
206 edge and incorporates adaptive temperature scaling for task-specific distillation. The student is opti-  
207 mized using a multi-objective loss function combining cross-entropy, MSE, KD, and contrastive  
208 losses. This architecture is designed to handle complex, cross-domain user utterances in low-  
209 resource Indic languages effectively. The total student loss function is defined as:

$$211 \quad \mathcal{L}_{\text{total}} = \alpha (\mathcal{L}_{\text{CE}}^{\text{ID}} + \mathcal{L}_{\text{KD}}^{\text{ID}}) + \beta (\mathcal{L}_{\text{CE}}^{\text{DC}} + \mathcal{L}_{\text{KD}}^{\text{DC}}) + \\ 212 \quad \gamma (\mathcal{L}_{\text{CE}}^{\text{SF}} + \mathcal{L}_{\text{KD}}^{\text{SF}} + \mathcal{L}_{\text{MSE}}^{\text{SF}} + \mathcal{L}_{\text{CRD}}^{\text{SF}}) \quad (4)$$

213 Where  $\alpha, \beta, \gamma$  controls the relative weighting across all loss components for a given task in the  
214 joint objective function

216  
217  
218 Table 1: Performance of multitask teacher models used for KD.  
219  
220  
221  
222

Model	Eval Loss	ID		DC		SF	
		Acc.	F1	Acc.	F1	Acc.	F1
Teacher 1 (IDSF)	0.4806	89.14	87.02	—	—	79.85	77.73
Teacher 2 (IDDC)	0.5195	80.07	77.28	90.00	89.77	—	—
Teacher 3 (DCSF)	0.0723	—	—	79.71	78.47	90.64	90.69

223  
224 4.2.1 STATIC QUANTIZATION APPLIED TO THE DISTILLED MODEL  
225226 We applied the similar static quantization techniques as applied in the baseline model and evaluate  
227 the results on cross-domain, multi-intent NLU. However, experiments conducted using static PTQ  
228 degraded performance due to disrupted KD signals, absence of quantization-aware training, and  
229 poor approximation of multilingual, multi-modal representations using min/max scaling.  
230231 4.2.2 DYNAMIC QUANTIZATION APPLIED TO THE DISTILLED MODEL  
232233 Rather than quantizing activations, we apply dynamic PTQ post-distillation to every `nn.Linear`  
234 layer in the student model corresponding to the weight matrices  
235

236 
$$W_{\text{intent}}, W_{\text{domain}}, W_{\text{slot}}, \text{linear projections}$$

237 For each weight  $W \in \mathbb{R}^{d_{\text{in}} \times d_{\text{out}}}$ , we compute:  
238

239 
$$s_W = \frac{\max |W|}{127}, \quad \widehat{W} = \text{round} \left( \frac{W}{s_W} \right) \quad (\text{int8}) \quad (5)$$
  
240

241 so that at inference time:  
242

243 
$$Wx \approx s_W (\widehat{W}x) \quad (6)$$

244 where  $x$  is the float32 input. Activations remain in float32 and are quantized on the fly. By leaving  
245  $\{H^{\text{CLS}}, H^i\}$  untouched during KD and quantizing only the linear mappings via Eqs. (11)–(12),  
246 we preserve the integrity of all losses— $\mathcal{L}_{\text{KD}}$ ,  $\mathcal{L}_{\text{MSE}}$ ,  $\mathcal{L}_{\text{CE}}$ , and  $\mathcal{L}_{\text{CRD}}$ —while achieving approximately.  
247248 4.2.3 PRECISION-CONTROLLED TASK SPECIFIC PTQ  
249250 To further improve efficiency while maintaining high accuracy, we propose a novel **Precision-  
251 Controlled Task Specific PTQ** framework applied to the distilled student model. The detailed PTQ  
252 architecture is explained in Fig. 2. Unlike conventional dynamic PTQ, which uniformly applies  
253 INT8 quantization to all linear layers, our method employs a *precision controller* to dynamically  
254 assign mixed-precision bit-widths  $\{4, 8, 16\}$  across different components of the network. Separate  
255 precision levels are selected for (i) encoder attention projections, (ii) encoder MLP/linear layers,  
256 and (iii) task-specific heads ( $W_{\text{intent}}, W_{\text{domain}}, W_{\text{slot}}$ ). Given a hidden representation  $H$  and a chosen  
257 bit-width  $b \in \{4, 8, 16\}$ , we define the integer range as:  
258

259 
$$q_{\min} = -2^{(b-1)}, \quad q_{\max} = 2^{(b-1)} - 1 \quad (7)$$

260 with scale factor:  
261

262 
$$s = \frac{\max(|H|)}{q_{\max}}. \quad (8)$$

263 The quantized tensor is obtained as:  
264

265 
$$\widehat{H} = \text{clip} \left( \text{round} \left( \frac{H}{s} \right), q_{\min}, q_{\max} \right) \cdot s. \quad (9)$$

266 Bit-widths are chosen by a lightweight controller that samples from a learned categorical distribution:  
267

268 
$$p(b | L) = \text{Softmax} \left( \frac{\theta_L + g}{\tau} \right), \quad (10)$$
  
269

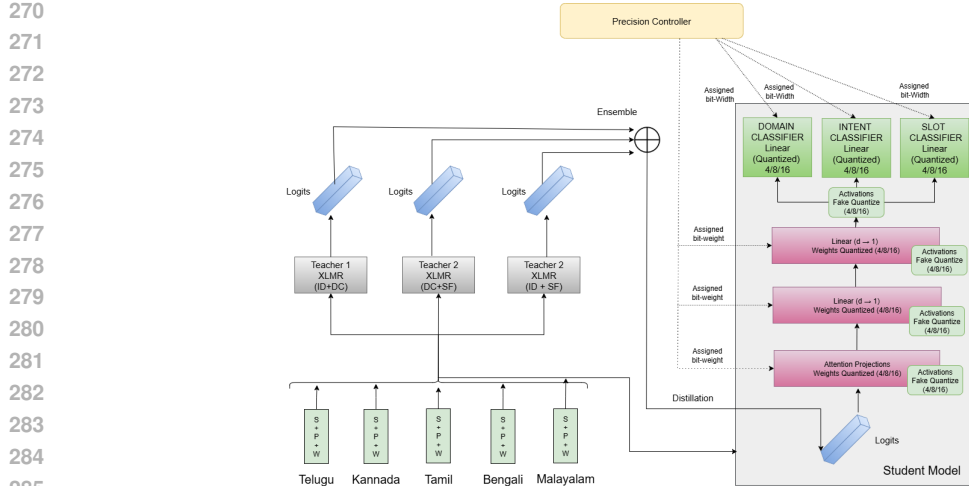


Figure 2: Precision Controlled Task Specific Dynamic PTQ

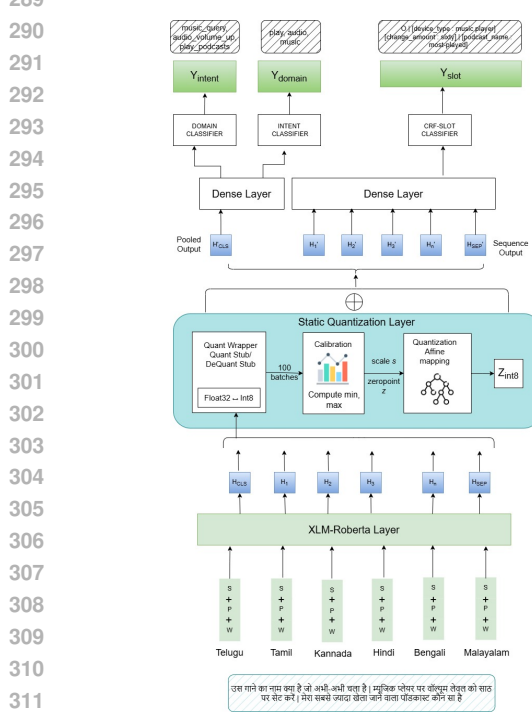


Figure 3: Static PTQ on Baseline Model

312  
313  
314  
315  
316  
317  
318  
319  
320  
321  
322  
323

where  $\theta_L$  are trainable logits for each layer  $L$ ,  $\tau$  is a temperature parameter, and  $g$  denotes Gumbel noise for exploration. Once the optimal assignment is identified, precisions are fixed and deployed deterministically. All targeted weights are permanently stored in compact INT4/INT8/INT16 form, reducing memory footprint, while activations are fake-quantized at runtime under the same precision policy. This unified control of weights and activations allows significant compression and bandwidth reduction, without degrading knowledge distillation signals. Empirically, our Precision-Controlled PTQ consistently outperforms both static and conventional dynamic PTQ, achieving the best trade-off between model size, inference latency, and task-level accuracy.

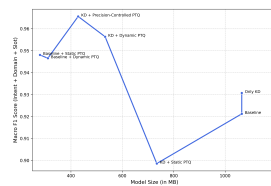


Figure 4: Model Size and Accuracy Tradeoff

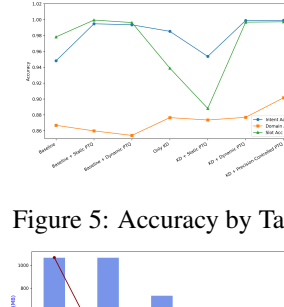


Figure 5: Accuracy by Task

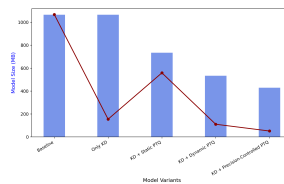


Figure 6: Efficiency Tradeoff

---

324 **Algorithm 1** Precision-Controlled Task Specific PTQ

---

325 1: **Input:** Pre-trained student model  $\mathcal{S}$ , teacher models  $\{\mathcal{T}_1, \mathcal{T}_2, \mathcal{T}_3\}$ , calibration dataset  $\mathcal{D}$ , candidate bit-widths  $\mathcal{Q} = \{4, 6, 8\}$ , trade-off parameter  $\alpha$

326 2: **Output:** Quantized student model  $\mathcal{S}_q$

327 3: Initialize precision controller  $C$  with random parameters

328 4: Collect layer-wise activation statistics on  $\mathcal{D}$

329 5: **for** each calibration batch  $B$  in  $\mathcal{D}$  **do**

330 6: Generate soft targets by fusing outputs of teacher models

331 7: **for** each layer  $l$  in student model  $\mathcal{S}$  **do**

332 8: Compute sensitivity score  $s_l$  based on weight and activation variance

333 9: Determine optimal bit-width using controller:

334

$$b_l = \arg \max_{q \in \mathcal{Q}} P(q|s_l, \alpha)$$

335

336 10: Quantize weights and activations of layer  $l$  to  $b_l$  bits

337 11: **end for**

338 12: Calculate distillation loss between teacher outputs and quantized model

339 13: Update  $\mathcal{S}$  and controller  $C$  using backpropagation

340 14: **end for**

341 15: Freeze bit-width assignments and export final quantized model  $\mathcal{S}_q = 0$

342

## 5 EXPERIMENTS

For all architectures, we used Python-based libraries such as PyTorch, Transformers along with statistical computing packages and open-source embedding models. Our baseline model fine-tuned XLM-RoBERTa-Base on a custom Indic dataset using the Adam optimizer with a learning rate of  $2 \times 10^{-5}$ , batch size of 32, and 5 training epochs. A linear scheduler with 10% warm-up followed by linear decay was used across `len(train_dataloader) × 5` steps. We applied cross-entropy loss for ID, DC, SF using a Conditional Random Field (CRF) layer for SF. We applied symmetric 8-bit PTQ with zero-point encoding and 256-batch calibration using QuantStub/DeQuantStub. In the Distillation setup, We distilled a single student model using offline distillation from three fine-tuned XLM-RoBERTa-Base multitask teachers (ID+DC, DC+SF, ID+SF) using a combination loss functions, with temperature scaling (4.0 utterance, 8.0 token) and loss weights (ID = 0.6, DC = 0.8, SF = 0.5). Training ran for 2 epochs with AdamW ( $lr = 3 \times 10^{-5}$ , batch size = 32). The resulting “Only KD” model matches the full-precision footprint (1064.86 MB), cuts CPU inference in half (92.20s), and improves task performance over the baseline. In the KD + Static PTQ setup, we wrapped the same distilled student in QuantStub/DeQuantStub modules and applied static PTQ: symmetric per-tensor 8-bit quantization (weights + activations) calibrated over 256 representative batches. No further retraining was needed. The resulting INT8 model (734.09 MB) 2x smaller in size—with a modest latency increase, while preserving accuracy.

In the KD + Dynamic PTQ setup, we quantized all linear and embedding layers of the already-distilled student. This hybrid approach produces an all-INT8 model that loads weights as int8 and computes activation scales on the fly. It achieves the best resource profile (533.12 MB) and fastest CPU inference (85.40s) over the FP32 baseline—while maintaining over the original model’s accuracy. To further enhance model efficiency, our KD + Precision Controlled Task Specific Dynamic PTQ augments the distilled student with precision-aware quantization policies tailored to each task head. This results in the most efficient trade-off between compression, speed, and accuracy. The proposed model achieves a footprint of 428.25 MB with the fastest CPU inference time of 76.34s. Importantly, it surpasses all prior variants in task performance, achieving near-perfect scores across metrics especially on the DC.

## 6 RESULTS AND ANALYSIS

This section discusses the results obtained across different experimental setups. Table 2 summarizes the performance metrics across the evaluated architectures, while Table 1 reports the performance

378  
379  
380  
381  
382 Table 2: Performance of baseline and distilled models under static, dynamic, and our proposed  
383 precision-controlled PTQ.  
384  
385  
386  
387

Model	Model Size (MB)	Inference Time (s)	Intent		Domain		Slot	
			Acc.	F1	Acc.	F1	Acc.	F1
Baseline Model	1064.80	232.24	0.9481	0.9373	0.8668	0.8590	0.9782	0.9674
Baseline Model + Static PTQ	279.58	99.57	0.9947	0.9939	0.8598	0.8509	0.9994	0.9994
Baseline Model + Dynamic PTQ	310.24	91.63	0.9934	0.9926	0.8541	0.8510	0.9962	0.9961
Only KD	1064.86	92.20	0.9852	0.9838	0.8765	0.8734	0.9388	0.9350
KD + Static PTQ	734.09	154.16	0.9536	0.9432	0.8735	0.8783	0.8881	0.8743
KD + Dynamic PTQ	533.12	85.40	0.9988	0.9985	0.8769	0.8742	0.9967	0.9964
<b>KD + Precision-Controlled PTQ (Ours)</b>	<b>428.25</b>	<b>76.34</b>	<b>0.9991</b>	<b>0.9989</b>	<b>0.9015</b>	<b>0.9010</b>	<b>0.9972</b>	<b>0.9969</b>

388  
389  
390 of the multitask teacher models. KD from the full-precision multitask teachers to a smaller student  
391 model enhanced with adaptive temperature scaling and contrastive learning for slot filling—achieved  
392 a 60.3% reduction in latency compared to the baseline. On this distilled model, we tested both  
393 static and dynamic PTQ. As shown in Table 2, applying static PTQ reduced model size by 31% but  
394 introduced additional inference overhead. Hence, we assessed dynamic PTQ in terms of size, speed,  
395 and accuracy. The KD + Dynamic PTQ setup achieved a 49.9% model size reduction, 63.2% faster  
396 inference, and near-perfect accuracy and F1 scores across ID, DC, and SF tasks.  
397398  
399  
400  
401  
402  
403  
404  
405  
406  
407 To further enhance inference time and maintain high accuracy, we applied our Precision-Controlled  
408 PTQ on the distilled student model. This approach strategically assigns low-precision weights across  
409 tasks without compromising performance. Compared to the baseline, the KD + Precision-Controlled  
410 Task Specific PTQ model achieved a 59.8% reduction in model size and a 67.1% faster inference,  
411 while delivering near-perfect accuracy and F1 scores across (ID: 99.91 / 99.89), (DC: 90.15 / 90.10),  
412 and (SF: 99.72 / 99.69) tasks. These results demonstrate that our approach effectively balances  
413 model size, inference speed and task accuracy, making it a highly practical solution for deploying  
414 high-performance NLU models on resource-constrained devices. Following our overall results for  
415 per-language performance in Table 3 and statistical significance in Table 4. The detailed results on  
416 model size vs accuracy tradeoff for all the architectures are explained in Fig. 4. Fig. 5 explains the  
417 accuracy for all the NLU tasks whereas, Fig. 6 illustrates the efficiency model size trade-off for all  
418 the architectures.419  
420  
421  
422  
423  
424  
425  
426  
427  
428  
429  
430  
431 **Per-Language Performance** We evaluate the KD + Precision-Controlled Task Specific PTQ  
427 model across six Indic languages (Hindi, Tamil, Telugu, Kannada, Malayalam, Bengali). As shown  
428 in Table 3, performance remains consistently high for the 3 NLU tasks. These results affirm the  
429 robustness and generalization of our model across diverse linguistic structures while preserving  
430 near-perfect intent, domain and slot detection performance.  
431440  
441  
442  
443  
444 Table 3: Per-language performance of KD + Precision-Controlled PTQ (Ours) on six Indic lan-  
445 guages.  
446

Language	Intent Acc	Intent F1	Domain Acc	Domain F1	Slot Acc	Slot F1
Hindi	0.9991	0.9989	0.9050	0.9040	0.9973	0.9971
Tamil	0.9988	0.9986	0.9020	0.9010	0.9970	0.9969
Kannada	0.9989	0.9987	0.9000	0.8990	0.9969	0.9967
Malayalam	0.9987	0.9985	0.8980	0.8970	0.9968	0.9966
Bengali	0.9990	0.9988	0.8995	0.8985	0.9969	0.9967
Telugu	0.9989	0.9987	0.9015	0.9005	0.9971	0.9969

447  
448  
449  
450  
451  
452  
453  
454  
455  
456  
457  
458  
459  
460  
461  
462  
463  
464  
465  
466  
467  
468  
469  
470  
471  
472  
473  
474  
475  
476  
477  
478  
479  
480  
481  
482  
483  
484  
485  
486  
487  
488  
489  
490  
491  
492  
493  
494  
495  
496  
497  
498  
499  
500  
501  
502  
503  
504  
505  
506  
507  
508  
509  
510  
511  
512  
513  
514  
515  
516  
517  
518  
519  
520  
521  
522  
523  
524  
525  
526  
527  
528  
529  
530  
531  
532  
533  
534  
535  
536  
537  
538  
539  
540  
541  
542  
543  
544  
545  
546  
547  
548  
549  
550  
551  
552  
553  
554  
555  
556  
557  
558  
559  
560  
561  
562  
563  
564  
565  
566  
567  
568  
569  
570  
571  
572  
573  
574  
575  
576  
577  
578  
579  
580  
581  
582  
583  
584  
585  
586  
587  
588  
589  
590  
591  
592  
593  
594  
595  
596  
597  
598  
599  
600  
601  
602  
603  
604  
605  
606  
607  
608  
609  
610  
611  
612  
613  
614  
615  
616  
617  
618  
619  
620  
621  
622  
623  
624  
625  
626  
627  
628  
629  
630  
631  
632  
633  
634  
635  
636  
637  
638  
639  
640  
641  
642  
643  
644  
645  
646  
647  
648  
649  
650  
651  
652  
653  
654  
655  
656  
657  
658  
659  
660  
661  
662  
663  
664  
665  
666  
667  
668  
669  
670  
671  
672  
673  
674  
675  
676  
677  
678  
679  
680  
681  
682  
683  
684  
685  
686  
687  
688  
689  
690  
691  
692  
693  
694  
695  
696  
697  
698  
699  
700  
701  
702  
703  
704  
705  
706  
707  
708  
709  
710  
711  
712  
713  
714  
715  
716  
717  
718  
719  
720  
721  
722  
723  
724  
725  
726  
727  
728  
729  
730  
731  
732  
733  
734  
735  
736  
737  
738  
739  
740  
741  
742  
743  
744  
745  
746  
747  
748  
749  
750  
751  
752  
753  
754  
755  
756  
757  
758  
759  
760  
761  
762  
763  
764  
765  
766  
767  
768  
769  
770  
771  
772  
773  
774  
775  
776  
777  
778  
779  
780  
781  
782  
783  
784  
785  
786  
787  
788  
789  
790  
791  
792  
793  
794  
795  
796  
797  
798  
799  
800  
801  
802  
803  
804  
805  
806  
807  
808  
809  
810  
811  
812  
813  
814  
815  
816  
817  
818  
819  
820  
821  
822  
823  
824  
825  
826  
827  
828  
829  
830  
831  
832  
833  
834  
835  
836  
837  
838  
839  
840  
841  
842  
843  
844  
845  
846  
847  
848  
849  
850  
851  
852  
853  
854  
855  
856  
857  
858  
859  
860  
861  
862  
863  
864  
865  
866  
867  
868  
869  
870  
871  
872  
873  
874  
875  
876  
877  
878  
879  
880  
881  
882  
883  
884  
885  
886  
887  
888  
889  
890  
891  
892  
893  
894  
895  
896  
897  
898  
899  
900  
901  
902  
903  
904  
905  
906  
907  
908  
909  
910  
911  
912  
913  
914  
915  
916  
917  
918  
919  
920  
921  
922  
923  
924  
925  
926  
927  
928  
929  
930  
931  
932  
933  
934  
935  
936  
937  
938  
939  
940  
941  
942  
943  
944  
945  
946  
947  
948  
949  
950  
951  
952  
953  
954  
955  
956  
957  
958  
959  
960  
961  
962  
963  
964  
965  
966  
967  
968  
969  
970  
971  
972  
973  
974  
975  
976  
977  
978  
979  
980  
981  
982  
983  
984  
985  
986  
987  
988  
989  
990  
991  
992  
993  
994  
995  
996  
997  
998  
999  
1000  
1001  
1002  
1003  
1004  
1005  
1006  
1007  
1008  
1009  
10010  
10011  
10012  
10013  
10014  
10015  
10016  
10017  
10018  
10019  
10020  
10021  
10022  
10023  
10024  
10025  
10026  
10027  
10028  
10029  
10030  
10031  
10032  
10033  
10034  
10035  
10036  
10037  
10038  
10039  
10040  
10041  
10042  
10043  
10044  
10045  
10046  
10047  
10048  
10049  
10050  
10051  
10052  
10053  
10054  
10055  
10056  
10057  
10058  
10059  
10060  
10061  
10062  
10063  
10064  
10065  
10066  
10067  
10068  
10069  
10070  
10071  
10072  
10073  
10074  
10075  
10076  
10077  
10078  
10079  
10080  
10081  
10082  
10083  
10084  
10085  
10086  
10087  
10088  
10089  
10090  
10091  
10092  
10093  
10094  
10095  
10096  
10097  
10098  
10099  
100100  
100101  
100102  
100103  
100104  
100105  
100106  
100107  
100108  
100109  
100110  
100111  
100112  
100113  
100114  
100115  
100116  
100117  
100118  
100119  
100120  
100121  
100122  
100123  
100124  
100125  
100126  
100127  
100128  
100129  
100130  
100131  
100132  
100133  
100134  
100135  
100136  
100137  
100138  
100139  
100140  
100141  
100142  
100143  
100144  
100145  
100146  
100147  
100148  
100149  
100150  
100151  
100152  
100153  
100154  
100155  
100156  
100157  
100158  
100159  
100160  
100161  
100162  
100163  
100164  
100165  
100166  
100167  
100168  
100169  
100170  
100171  
100172  
100173  
100174  
100175  
100176  
100177  
100178  
100179  
100180  
100181  
100182  
100183  
100184  
100185  
100186  
100187  
100188  
100189  
100190  
100191  
100192  
100193  
100194  
100195  
100196  
100197  
100198  
100199  
100200  
100201  
100202  
100203  
100204  
100205  
100206  
100207  
100208  
100209  
100210  
100211  
100212  
100213  
100214  
100215  
100216  
100217  
100218  
100219  
100220  
100221  
100222  
100223  
100224  
100225  
100226  
100227  
100228  
100229  
100230  
100231  
100232  
100233  
100234  
100235  
100236  
100237  
100238  
100239  
100240  
100241  
100242  
100243  
100244  
100245  
100246  
100247  
100248  
100249  
100250  
100251  
100252  
100253  
100254  
100255  
100256  
100257  
100258  
100259  
100260  
100261  
100262  
100263  
100264  
100265  
100266  
100267  
100268  
100269  
100270  
100271  
100272  
100273  
100274  
100275  
100276  
100277  
100278  
100279  
100280  
100281  
100282  
100283  
100284  
100285  
100286  
100287  
100288  
100289  
100290  
100291  
100292  
100293  
100294  
100295  
100296  
100297  
100298  
100299  
100300  
100301  
100302  
100303  
100304  
100305  
100306  
100307  
100308  
100309  
100310  
100311  
100312  
100313  
100314  
100315  
100316  
100317  
100318  
100319  
100320  
100321  
100322  
100323  
100324  
100325  
100326  
100327  
100328  
100329  
100330  
100331  
100332  
100333  
100334  
100335  
100336  
100337  
100338  
100339  
100340  
100341  
100342  
100343  
100344  
100345  
100346  
100347  
100348  
100349  
100350  
100351  
100352  
100353  
100354  
100355  
100356  
100357  
100358  
100359  
100360  
100361  
100362  
100363  
100364  
100365  
100366  
100367  
100368  
100369  
100370  
100371  
100372  
100373  
100374  
100375  
100376  
100377  
100378  
100379  
100380  
100381  
100382  
100383  
100384  
100385  
100386  
100387  
100388  
100389  
100390  
100391  
100392  
100393  
100394  
100395  
100396  
100397  
100398  
100399  
100400  
100401  
100402  
100403  
100404  
100405  
100406  
100407  
100408  
100409  
100410  
100411  
100412  
100413  
100414  
100415  
100416  
100417  
100418  
100419  
100420  
100421  
100422  
100423  
100424  
100425  
100426  
100427  
100428  
100429  
100430  
100431  
100432  
100433  
100434  
100435  
100436  
100437  
100438  
100439  
100440  
100441  
100442  
100443  
100444  
100445  
100446  
100447  
100448  
100449  
100450  
100451  
100452  
100453  
100454  
100455  
100456  
100457  
100458  
100459  
100460  
100461  
100462  
100463  
100464  
100465  
100466  
100467  
100468  
100469  
100470  
100471  
100472  
100473  
100474  
100475  
100476  
100477  
100478  
100479  
100480  
100481  
100482  
100483  
100484  
100485  
100486  
100487  
100488  
100489  
100490  
100491  
100492  
100493  
100494  
100495  
100496  
100497  
100498  
100499  
100500  
100501  
100502  
100503  
100504  
100505  
100506  
100507  
100508  
100509  
100510  
100511  
100512  
100513  
100514  
100515  
100516  
100517  
100518  
100519  
100520  
100521  
100522  
100523  
100524  
100525  
100526  
100527  
100528  
100529  
100530  
100531  
100532  
100533  
100534  
100535  
100536  
100537  
100538  
100539  
100540  
100541  
100542  
100543  
100544  
100545  
100546  
100547  
100548  
100549  
100550  
100551  
100552  
100553  
100554  
100555  
100556  
100557  
100558  
100559  
100560  
100561  
100562  
100563  
100564  
100565  
100566  
100567  
100568  
100569  
100570  
100571  
100572  
100573  
100574  
100575  
100576  
100577  
100578  
100579  
100580  
100581  
100582  
100583  
100584  
100585  
100586  
100587  
100588  
100589  
100590  
100591  
100592  
100593  
100594  
100595  
100596  
100597  
100598  
100599  
100600  
100601  
100602  
100603  
100604  
100605  
100606  
100607  
100608  
100609  
100610  
100611  
100612  
100613  
100614  
100615  
100616  
100617  
100618  
100619  
100620  
100621  
100622  
100623  
100624  
100625  
100626  
100627  
100628  
100629  
100630  
100631  
100632  
100633  
100634  
100635  
100636  
100637  
100638  
100639  
100640  
100641  
100642  
100643  
100644  
100645  
100646  
100647  
100648  
100649  
100650  
100651  
100652  
100653  
100654  
100655  
100656  
100657  
100658  
100659  
100660  
100661  
100662  
100663  
100664  
100665  
100666  
100667  
100668  
100669  
100670  
100671  
100672  
100673  
100674  
100675  
100676  
100677  
100678  
100679  
100680  
100681  
100682  
100683  
100684  
100685  
100686  
100687  
100688  
100689  
100690  
100691  
100692  
100693  
100694  
100695  
100696

432 these findings confirm that our precision-controlled quantization strategy not only reduces model  
 433 size and inference time but also delivers significant accuracy gains in challenging tasks like ID and  
 434 DC, highlighting its robustness and effectiveness for multilingual NLU.  
 435

436 Table 4: Statistical comparison of Baseline + Static PTQ and KD + Precision-Controlled PTQ across  
 437 key NLU metrics.

Metric	Baseline + Static PTQ	KD + Precision-Controlled PTQ	p-value
Intent Accuracy	$0.9947 \pm 0.0021$	$0.9991 \pm 0.0006$	< 0.001
Intent F1	$0.9939 \pm 0.0024$	$0.9989 \pm 0.0007$	< 0.001
Domain Accuracy	$0.8598 \pm 0.0153$	$0.9015 \pm 0.0085$	0.010
Domain F1	$0.8509 \pm 0.0171$	$0.9010 \pm 0.0090$	0.015
Slot Accuracy	$0.9994 \pm 0.0005$	$0.9972 \pm 0.0010$	0.080
Slot F1	$0.9994 \pm 0.0005$	$0.9969 \pm 0.0011$	0.070

## 448 7 ERROR ANALYSIS

449  
 450 Based on our experiments, we find that SF is the most sensitive to quantization noise, followed  
 451 by ID. DC, being a coarser-grained task, demonstrates relatively higher robustness under quantized  
 452 settings. In multilingual utterances containing multiple intents, the model frequently over predicts  
 453 domains, often adding unrelated domains such as alarm or email in music-centric inputs, particularly  
 454 in Malayalam and Bengali. This behavior reflects in multi-domain disentanglement under quantized  
 455 constraints. We also observe that Dravidian languages such as Malayalam and Tamil exhibit higher  
 456 rates of domain mis-classification, which we attribute to richer morphology, longer sentence struc-  
 457 tures, and limited training resources in these languages. Additionally, we notice frequent confusion  
 458 between semantically similar intents, such as music\_query versus play\_music and calendar\_query  
 459 versus calendar\_set, especially in Malayalam and Tamil. This suggests insufficient separation in the  
 460 learned intent embedding space when operating under quantized precision. Importantly, when com-  
 461 paring both models, we find that the dynamically quantized model demonstrates fewer such errors  
 462 than the static PTQ baseline. This supports our design decision to apply multi-teacher distillation  
 463 prior to quantization, which enhances task separation and allows for greater numerical flexibility  
 464 during downstream execution.

## 465 8 CONCLUSION

466 This study demonstrates that a low-precision distilled student model can substantially reduce both  
 467 latency and model size while maintaining, and in some cases improving, accuracy across ID, DC  
 468 and SF tasks. By leveraging adaptive attention fusion and temperature scaling, the approach delivers  
 469 real-time, scalable performance on constrained hardware. Although static PTQ provides compres-  
 470 sion benefits for cross-domain, multi-intent NLU in low-resource Indic languages, its inference  
 471 overhead limits practical utility. In contrast, integrating multitask, multi-teacher KD with dynamic  
 472 PTQ achieves a more effective balance of efficiency and accuracy, yielding significant reductions  
 473 in model size and latency without compromising task performance. Extending this further, our  
 474 precision-controlled, task-specific dynamic PTQ framework unifies weight-activation quantization  
 475 under a controller-driven policy, allowing fine-grained precision assignment across encoder layers  
 476 and task heads. This achieves the most favorable trade-off, with up to 59.8% model size reduc-  
 477 tion and 67.1% faster inference, while sustaining near-perfect accuracy across ID, DC, and SF.  
 478 Overall, the combination of multitask, multi-teacher KD and precision-controlled task specific PTQ  
 479 provides a scalable, resource-efficient, and high-performance solution for deploying multilingual  
 480 cross-domain, multi-intent NLU systems in low-resource, on-device environments.  
 481

482 **Limitations** While our KD + PTQ framework demonstrates strong performance and efficiency on  
 483 low-resource Indic NLU tasks, two key limitations remain. The approach relies solely on PTQ  
 484 (static/dynamic) and does not incorporate QAT, which could enhance robustness under aggressive  
 485 quantization in low-resource cross-domain settings. Future work could explore pruning and related  
 486 compression techniques to further reduce model size.

486 REFERENCES  
487

488 Zhen Dong, Zhewei Yao, Daiyaan Arfeen, Amir Gholami, Michael W Mahoney, and Kurt Keutzer.  
489 Hawq-v2: Hessian aware trace-weighted quantization of neural networks. *Advances in neural*  
490 *information processing systems*, 33:18518–18529, 2020.

491 Yousef El-Kurdi, Jerry Quinn, and Avirup Sil. Zero-shot dynamic quantization for transformer  
492 inference. *arXiv preprint arXiv:2211.09744*, 2022.

493 Elias Frantar, Saleh Ashkboos, Torsten Hoefer, and Dan Alistarh. Gptq: Accurate post-training  
494 quantization for generative pre-trained transformers. *arXiv preprint arXiv:2210.17323*, 2022.

495

496 Geoffrey Hinton, Oriol Vinyals, and Jeff Dean. Distilling the knowledge in a neural network. *arXiv*  
497 *preprint arXiv:1503.02531*, 2015.

498

499 Qiang Hu, Yuejun Guo, Xiaofei Xie, Maxime Cordy, Mike Papadakis, Lei Ma, and Yves Le Traon.  
500 Aries: Efficient testing of deep neural networks via labeling-free accuracy estimation. In *2023*  
501 *IEEE/ACM 45th International Conference on Software Engineering (ICSE)*, pp. 1776–1787.  
502 IEEE, 2023.

503 Charith Peris Scott Mackie Kay Rottmann Ana Sanchez Aaron Nash Liam Urbach Vishesh Kakar-  
504 ala Richa Singh Swetha Ranganath Laurie Crist Misha Britan Wouter Leeuwis Gokhan Tur  
505 Prem Natarajan Jack FitzGerald, Christopher Hench. Massive: A 1m-example multilingual nat-  
506 ural language understanding dataset with 51 typologically-diverse languages. *arXiv:2204.08582*,  
507 2022.

508

509 Sangil Jung, Changyong Son, Seohyung Lee, Jinwoo Son, Jae-Joon Han, Youngjun Kwak, Sung Ju  
510 Hwang, and Changkyu Choi. Learning to quantize deep networks by optimizing quantization  
511 intervals with task loss. In *Proceedings of the IEEE/CVF conference on computer vision and*  
512 *pattern recognition*, pp. 4350–4359, 2019.

513

514 Jiedong Lang, Zhehao Guo, and Shuyu Huang. A comprehensive study on quantization tech-  
515 niques for large language models. In *2024 4th International Conference on Artificial Intelligence,*  
516 *Robotics, and Communication (ICAIRC)*, pp. 224–231. IEEE, 2024.

517

518 Yan Li, So-Eon Kim, Seong-Bae Park, and Soyeon Caren Han. Midas: Multi-level intent, domain,  
519 and slot knowledge distillation for multi-turn nlu. *arXiv preprint arXiv:2408.08144*, 2024.

520

521 Chengyuan Liu, Yangyan g Kang, Fubang Zhao, Kun Kuang, Zhuoren Jiang, Changlong Sun, and  
522 Fei Wu. Evolving knowledge distillation with large language models and active learning. *arXiv*  
523 *preprint arXiv:2403.06414*, 2024.

524

525 Navin Ranjan and Andreas Savakis. Vision transformer quantization with multi-step knowledge  
526 distillation. In *Signal Processing, Sensor/Information Fusion, and Target Recognition XXXIII*,  
527 volume 13057, pp. 283–292. SPIE, 2024.

528

529 Adriana Romero, Nicolas Ballas, Samira Ebrahimi Kahou, Antoine Chassang, Carlo Gatta, and  
530 Yoshua Bengio. Fitnets: Hints for thin deep nets. *arXiv preprint arXiv:1412.6550*, 2014.

531

532 Tulika Saha, Neeti Priya, Sriparna Saha, and Pushpak Bhattacharyya. A transformer based multi-  
533 task model for domain classification, intent detection and slot-filling. In *2021 International Joint*  
534 *Conference on Neural Networks (IJCNN)*, pp. 1–8, 2021.

535

536 Liyuan Sun, Jianping Gou, Baosheng Yu, Lan Du, and Dacheng Tao. Collaborative teacher-student  
537 learning via multiple knowledge transfer. *arXiv preprint arXiv:2101.08471*, 2021.

538

539 Kuan Wang, Zhijian Liu, Yujun Lin, Ji Lin, and Song Han. Haq: Hardware-aware automated quan-  
540 tization with mixed precision. In *Proceedings of the IEEE/CVF conference on computer vision*  
541 *and pattern recognition*, pp. 8612–8620, 2019.

542

543 Guangxuan Xiao, Ji Lin, Mickael Seznec, Hao Wu, Julien Demouth, and Song Han. Smoothquant:  
544 Accurate and efficient post-training quantization for large language models. In *International*  
545 *Conference on Machine Learning*, pp. 38087–38099. PMLR, 2023.

540 Hanqi Xiao, Yi-Lin Sung, Elias Stengel-Eskin, and Mohit Bansal. Task-circuit quantiza-  
541 tion: Leveraging knowledge localization and interpretability for compression. *arXiv preprint*  
542 *arXiv:2504.07389*, 2025.

543

544 Zhewei Yao, Reza Yazdani Aminabadi, Minjia Zhang, Xiaoxia Wu, Conglong Li, and Yuxiong  
545 He. Zeroquant: Efficient and affordable post-training quantization for large-scale transformers.  
546 *Advances in neural information processing systems*, 35:27168–27183, 2022.

547

548

549

550

551

552

553

554

555

556

557

558

559

560

561

562

563

564

565

566

567

568

569

570

571

572

573

574

575

576

577

578

579

580

581

582

583

584

585

586

587

588

589

590

591

592

593